2009
15) 鈴木裕子編：子どもの脳脊髄液減少症．日本医療企画，2007
16) 高橋浩一，美馬達夫：小児期に発症した脳脊髄液減少症9例の検討　—臨床像とその対応—．小児の脳神経 33:462-468，2008
17) 寺尾　亨，谷口　真，磯尾綾子：脳脊髄液減少症患者の髄液漏出部位の同定におけるCTミエログラフィーの有用性．脳脊髄液減少症データ集Vol.2．pp35-42，メディカルレビュー社，2009
18) Turnbull DK, Shepherd DB : Post-dural puncture headache: pathogenesis, prevention and treatment. British Journal of Anaesthesia 91(5):718-729, 2003

II

生理的髄液循環

ヒト成人の脳脊髄液は150～200mLとされ，1日当たり3回入れ替わるとされている．大部分の髄液は脳室内の脈絡叢から分泌され，主に上矢状静脈洞周辺のクモ膜顆粒から吸収される（図II-1）．クモ膜顆粒は海綿静脈洞など他の静脈洞にも存在するし，脊髄根静脈にも類似の構造物があることは以前から報告されている．早期膀胱内RI集積，RIクリアランスを診断基準とするには，脊髄レベルでの髄液吸収について考えておく必要がある．

図II-2のような模式図が知られているが，そのもとになる研究は1970年代のものである[2,4]．神経根部の経リンパ系吸収路も想定されており，脊髄レベルでの髄液吸収は，特に新しい概念ではない．

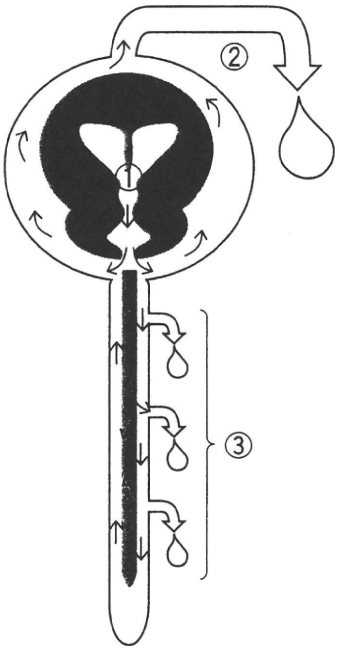

図II-1　脳脊髄液の産生～吸収の模式図
①脳脊髄液の大部分は，脳室内脈絡叢毛細管からの血漿の限外濾過液に由来するが，一部は脳，脊髄実質でも産生されると考えられている．②頭蓋内矢状静脈洞周辺のクモ膜顆粒が主な吸収経路とされるが，横静脈洞にもクモ膜顆粒が存在する．③脊髄神経根周辺にも同様の構造物がみられ，髄液吸収に関与すると考えられている．さらに脳神経，脊髄神経根では経リンパ系の吸収路の存在も証明されている．

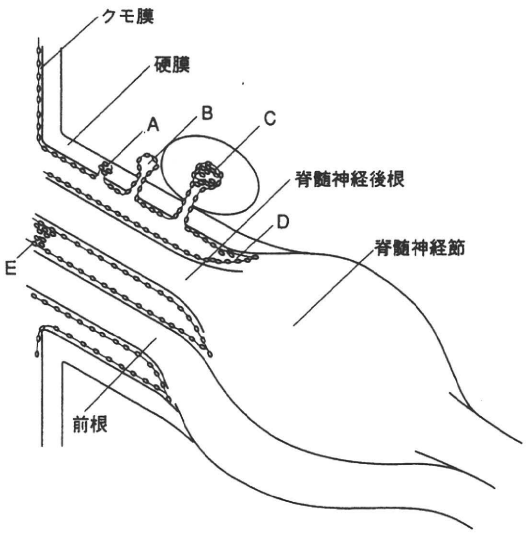

脊髄神経線維に沿って存在するarachnoid villiの構造
A：硬膜内にみられるarachnoid villi
B：arachnoid villiが硬膜を貫通して存在
C：arachnoid villiは脊髄静脈内に突出して存在
D，E：クモ膜下腔内にみられるarachnoid villi

図II-2　脊髄神経根周囲のクモ膜絨毛，クモ膜顆粒に関する従来の説明図[2]
（原典は文献4と思われる）

この研究は3体の屍体から取り出したTh1以下の脊髄，脊髄神経根を用いた研究であり現在でも十分に通用するレベルの高いものである[4]．脊髄クモ膜下腔を色素溶液で灌流し，濃染された神経根，あるいは太い静脈が表面にある神経根を選んで検討している．3体で胸椎，腰椎の神経根，総計102本のうち，26本を調べている．1本当たり2個近くのクモ膜絨毛組織が存在したとの結論であるが，76本は未調査なので正確な総数は不明である．大きさは最大でも，$5.43 \times 10^8\ \mu^3$であり，頭蓋内のクモ膜顆粒に比べると随分と小さい．図II-2のAのような硬膜内に存在するタイプが最も多く，このタイプの顆粒の大部分は灌流した色素を含んでいた．

最近の報告も，このデータを裏付けている[14]（図II-3）．この報告は，10体の屍体を用いているが，頸椎神経根を含めてすべての神経根を検索したさらに詳細な研究である．結論として，太い根静脈ほど周辺にたくさんの絨毛組織を持ち，頸椎レベルに2～3個，胸椎に3～4個，腰椎に5～6個（一側につき）であり，合計20～30個である．この報告では，図II-2のような分類はされていない．ほとんどのクモ膜絨毛は近接する根静脈にめり込むか，接していたと記載されている．

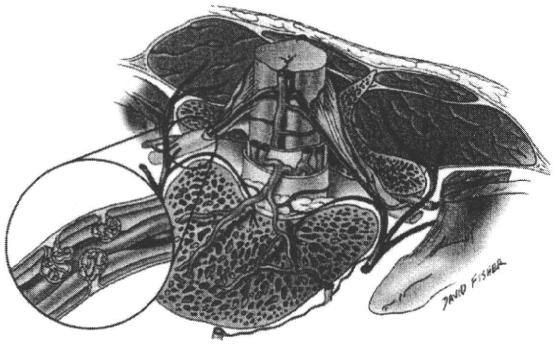

図II-3　ヒト脊髄神経根部のクモ膜顆粒[14]

これらの絨毛組織は50～170μm（平均100μm）であり，肉眼で確認できるほど大きいクモ膜顆粒はない．頭蓋内では横静脈洞のクモ膜顆粒が平均4mmの大きさであることを考えると，脊髄レベルのクモ膜絨毛を合わせても頭蓋内のクモ膜顆粒1個の大きさにも満たないことになる[5]．さらに上矢状静脈洞の前部には2mm以下の顆粒が無数にみられることも報告されている．神経根鞘外膜のfenestrationを通しての髄液の自由移動による吸収なども想定されてはいるが，クモ膜顆粒が髄液吸収の主役であるならば，脊髄レベルでの髄液吸収量は，頭蓋内に比し桁違いに少ないことになる．

根静脈の太さと，その周辺のクモ膜顆粒の有無，数が密接に関係するのであれば，結局根静脈の血流量に応じて，髄液が吸収されることになる．任意の根静脈の血流量は，その静脈が灌流する組織の体積に比例する．この理屈を全体に敷衍すれば，頭蓋内，脊柱管内の髄液吸収量は，脳と脊髄の血流量，さらには体積，重量に比例することになる．最近の研究では，脳～脊髄組織，静脈への直接の髄液吸収の可能性も挙げられている[13]．この場合にも，体積，重量に応じた髄液吸収量と考えるのが妥当であろう．日本人での脳は平均1216～1096g，脊髄は25.5～23.9gとされている[3]．脊髄レベルでは約1/40＝2.5%の髄液吸収ということになる．

われわれの定量的RICのデータから，脊髄レベルでの髄液吸収量の計算を試みた．2004年5月～2009年8月の間に，直接漏出所見，2.5時間以内の明らかな膀胱内RI集積，RI脳室内逆流がなく，正常髄液循環と判定した207例を対象として分析した．その中から2.5時間後にもRIが頭蓋内に流入せず，脊柱管内に留まっている15例と残りの192例を比較検討した（図II-4）．

このような例では1～2.5時間の減衰は，自然減衰（$e^{-0.01t}$）を除けば100%脊柱管内での髄液吸収に依存しているはずである．12例のこの区間のクリアランスは，$e^{-0.0128t}$であった．したがって，“0.0128－0.01＝0.0028”が脊柱管内の髄液吸収である．残りの192例では，この区間のクリアランスは有意に早く，$e^{-0.03677t}$であった．一方で，2.5時間後にはRIは髄液腔に広く拡散しており，

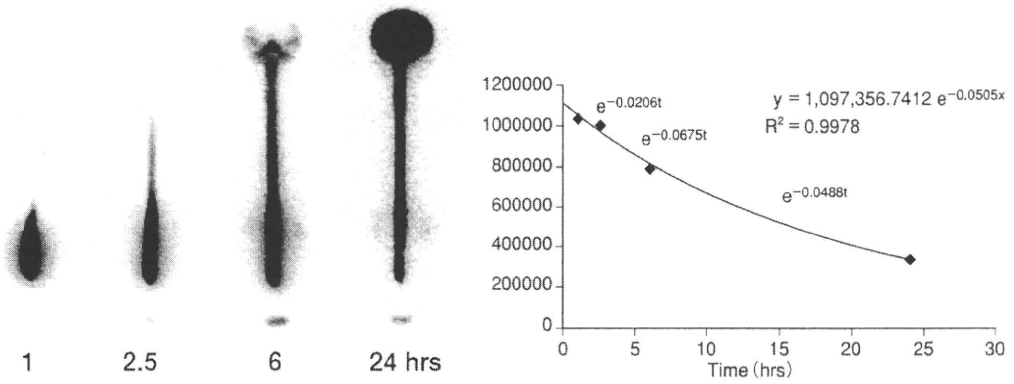

図 II-4　正常と判定された例の RIC 所見
41 歳男性．交通外傷後の頭痛，頸部痛などで受診，RIC で髄液漏なしと判定された．

以後のクリアランス値は，全脳脊髄液腔の髄液吸収をよく反映するはずである．0.0502 − 0.01 = 0.0402 がその値となる．クリアランス値は薬力動態学的には elimination rate constant に相当し，v/V（v：吸収される髄液量，V：RI が分布する髄液腔の容積）に一致する[6,7,12]．全髄液腔を 150mL，脳室容積を 30mL と仮定すれば，2.5 時間以降は V = 120mL となる．したがって，この区間では v = 120 × 0.0402 = 4.8mL/hr の髄液吸収となる．脊柱管内の髄液量を 50mL と仮定すれば，1 ～ 2.5 時間の吸収量は 50 × 0.0028 = 0.14mL となる．

以上の計算からは，脊柱管内の髄液吸収量は全体の 0.14/4.8 = 2.9% になる．先ほどの推測値 2.5% に近い値となる[11]．ただし，全体で 1 時間当たり 4.7mL の髄液吸収量との計算値は，1 日に約 500mL とされる現在の認識の約 1/4 であり，われわれの計算の絶対値には疑問の余地がある．しかし，「2.5 時間での RI の頭側への拡散が早い例ほど，1 ～ 2.5 時間のクリアランスが早い」ことだけでも，脊柱管内での髄液吸収が相対的に少ないことの十分な証拠であろう（図 II-5）．

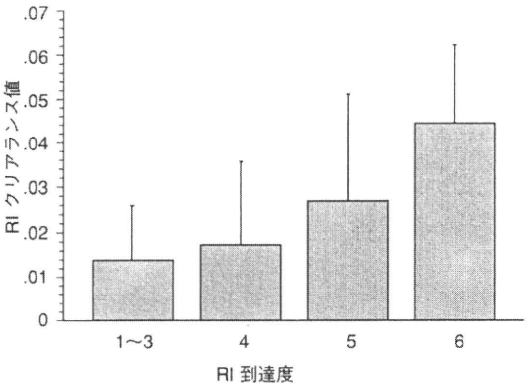

図 II-5　RI 到達度と RI クリアランス
正常髄液循環と判定した N 群の 1 ～ 2.5 時間の RI クリアランス値を，2.5 時間での RI 到達度により分類．頭側への RI 拡散が早いほど，RI の吸収が早いことを示している．RI 到達度，RI クリアランスについては本書 VI を参照．

この点については，われわれのデータと相反する研究がある[1]．健常人ボランティアを対象とした貴重なデータであるが，残念ながら方法論に重大な欠陥がある．RIC の方法はわれわれのものと類似しており，注入から 1 時間までの脊柱管内の RI 活性の減衰速度を計測している．1 時間までは頭蓋内に RI が流入しないとの仮定のもとに，頭蓋内の RI 活性を測定していない．その点についていくつかの根拠を挙げて，頭蓋内流入は無視できると考察している．しかし，1 時間では 40% 以上の例で，肉眼的に頭蓋内に RI が流入している[9,11]．したがって頭蓋内流入分が脊髄内吸収分に勘定され，脊髄レベルでの髄液吸収が過大評価されている可能性が高い．この研究で使われている 22G（おそらくランセット針）は，一定の針穴漏出が見込まれる（3.3mL/hr：O'Conor, 2007）．注入直後から歩行させた群では特に，針穴漏出分も脊髄内吸収分に含まれている可能性がある．

以上のように現時点での資料を客観的に分析すると，脊髄レベルでも髄液吸収が起こっていることは間違いない．しかし，その量は頭蓋内に比べて桁違いに少ないと考えられる．脊髄レベルでの

生理的髄液吸収により，3～4時間以内に尿中に排泄されるRIが存在するとしても量は少ないと思われる．また硬膜外ブラッドパッチ（EBP）が，この脊髄レベルでの吸収機構を障害する可能性が指摘されているが，脊髄レベルでの髄液吸収機構は硬膜内に存在するので，EBPにより髄液吸収が阻害されるとは考えられない[7,10,14,15,16]．EBPに関する論文にも，合併症，副作用の項目にこのような記載があるものを目にしたことはない．すでにEBP治療は40年以上の歴史があり，この指摘は杞憂と言うべきであろう．

参考文献

1）Edsbagge M, Tisell M, Jacobson L, et al: Spinal CSF absorption in healthy individuals. Am J Physiol Regul Integr Comp Physiol 287: R1450-R1455, 2004
2）林　隆士：神経系奇形の画像と臨床（12）．Medical Postgraduates 33(3):38-48, 1995
3）金光　晟：脊髄の解剖．臨床神経科学3(11):12-16, 1985
4）Kido DK, Gomez DG, Pavese AM Jr, Potts DG: Human spinal arachnoid villi and granulations. Neuroradiology 11:221-228, 1976
5）Liang L, Korogi Y, Sugahara T, Ikushima I, Shigematsu Y, Takahashi M, Provenzale JM: Normal structures in the intracranial dural sinuses: delineation with 3D contrast-enhanced magnetization prepared rapid acquisition gradient-echo imaging sequence. AJNR 23:1739-1746, 2002
6）Lying-Tunell U, Soderborg B: Quantitative scintigraphic method of estimating the circulation of cerebrospinal fluid. Acta Radiol Diagn (Stockh) 13: 554-569, 1972
7）美馬達夫：脳脊髄液減少症に関するさまざまな見解に対する私見．脳脊髄液減少症研究会ガイドライン作成委員会編：脳脊髄液減少症データ集2．pp117-121，メディカルレビュー社，2009
8）Moriyama E, Ogawa T, Nishida A, et al: Quantitative analysis of radioisotope cisternography in the diagnosis of intracranial hypotension. J Neurosurg 101:421-426, 2004
9）守山英二，寺田洋明：外傷性脳脊髄液減少症の臨床像と治療成績　脳脊髄液減少症ガイドライン2007．pp91-100，163-168，メディカルレビュー社，2007
10）守山英二，寺田洋明：外傷性脳脊髄液減少症をめぐる議論について：5年間の臨床経験から．脳脊髄液減少症研究会ガイドライン作成委員会編：脳脊髄液減少症データ集1．pp141-146，メディカルレビュー社，2007
11）守山英二，寺田洋明：RI脳槽造影による健常者髄液循環の検討：特に脊柱管内での髄液吸収について　第9回日本正常圧水頭症研究会　プロシーディング
12）Ritschel WA, Kearns GL: Handbook of Basic Pharmacokinetics. the American Pharmaceutical Association, 2004
13）谷　諭：脊椎管内における髄液循環動態　小児の脳神経 30:6-11, 2005
14）Tubbs RS, Hansasuta A, Stetler W, Kelly DR, Blevins D, Humphrey R, Chua GD, Shoja MM, Loukas M, Oakes WJ: Human spinal arachnoid villi revisited: immunohistological study and review of the literature. J Neurosurg Spine 7:328-331, 2007
15）吉本智信：低髄液圧症候群．自動車保険ジャーナル，2006
16）吉本智信：脳脊髄液減少症ガイドライン2007を巡る問題点．pp1-20，医研センタージャーナル，2007年8月号

薬剤情報　佐原英城

- メリスロンはヒスタミン類似作用があり，胃酸分泌亢進や気道収縮を起こすおそれがあるので，消化性潰瘍・気管支喘息患者には慎重に投与する必要がある．薬歴管理と服薬指導に際して留意し，必要時には医師に確認する．
- めまいに伴った悪心，嘔吐に使用するナウゼリンは動物実験（ラット）で骨格，内臓異常などの催奇形性が報告されているので，妊婦には投与禁忌である．服薬指導に際して留意する．
- メイロンは寒冷期に結晶が析出する場合がある．その場合は温めて結晶を溶解させてから使用すること．
- 「トラベルミン」という薬品名であっても，医療用と薬局で市販している薬（トラベルミンR，トラベルミンファミリー，トラベルミン内服液など）では含有成分が異なる場合がある．抗コリン薬を含有するものもあるので患者が混同して使用しないよう指導すること．

低髄液圧症候群

intracranial hypotension

佐藤慎哉　山形大学教授・総合医学教育センター

病態と診断

Ⓐ 病態

髄液の減少による髄液圧の低下や代償性の血管拡張，起立時の脳の下垂による脳の血管や神経の牽引により症状を呈する．

原因として，腰椎穿刺や硬膜損傷を伴う脊髄脊椎外傷，髄膜の嚢胞などが知られているが，原因が特定できず特発性とされる症例もある．髄液圧が正常範囲内の症例も報告され，脳脊髄液減少症ともよばれる．

Ⓑ 診断

起立性頭痛が特徴的で，ほかに項部硬直，耳鳴，聴力低下，光過敏，悪心を伴う場合もある．臨床症状に加え，造影頭部MRIでの硬膜下腔拡大，静脈拡張，小脳扁桃下垂，硬膜肥厚など髄液減少による間接所見や，RI脳槽造影，CTミエログラフィーによる髄液漏出の直接所見により診断する．

治療方針

髄液漏出部位の自然閉鎖を期待し，安静臥床が治療の基本である．髄液の減少に対しては，水分補給を行う．保存的治療が無効の場合，ブラッドパッチが行われる場合がある．

Ⓐ 保存的治療

2－3週間の安静臥床と経口摂取・補液を含め1日2L程度の水分補給を行う．

Ⓡ 処方例

ソルラクト注（500 mL）　1回1,500 mL　1日1回　点滴静注

Ⓑ 薬物療法

対症療法として，下記の薬剤を適宜用いる．カフェインは，血管拡張性頭痛に対しての処方である．コルチコステロイドが有効であるとの報告もあるが，確立した処方ではない．

Ⓡ 処方例　以下を適宜組み合わせて用いる．

1）デパス錠（0.5 mg）　3錠　分3 7
2）ロキソニン錠（60 mg）　3錠　分3 5
3）カフェイン末　1回0.3 g　頓用

Ⓒ ブラッドパッチ（硬膜外自己血注入法）

保存的治療では症状が改善せず，髄液漏の存在部位が明らかな場合，髄液漏出部の閉鎖を目的に，自己静脈血を硬膜外に注入する．注入量は部位により異なり，腰椎部では20－40 mL，頸椎・胸椎部では10－15 mL前後である．複数回行う場合は，3か月以上間隔をあける．本法の歴史は古いが，保険適用外の治療法であり，その適応は十分な検討を要す．

患者説明のポイント

- MRIやRI脳槽造影の画像診断基準は確立されておらず，現在，日本の関連する学会が協力してガイドラインを策定中である．
- ブラッドパッチは，決して安全な治療法ではなく，安易に行うべきものではない．
- 複数回のブラッドパッチが必要な場合や無効例もある．

脳血管障害による運動麻痺のリハビリテーション

rehabilitation for motor dysfunction due to cerebrovascular disorder

安保雅博　東京慈恵会医科大学主任教授・リハビリテーション医学講座

病態と診断

脳血管障害による一般的な中枢性麻痺の回復は，弛緩性完全麻痺→連合反応の出現→共同運動の出現→共同運動の完成→分離運動の出現→巧緻性の向上→スピードの正常化という過程をたどるが，出血量の少ない手術適応のない脳出血のように，数日の脳浮腫ならびに血腫の軽減に伴い，弛緩性完全麻痺から共同運動を経ないで分離運動ができるレベルまで

Acta Neurochir (2011) 153:437–438
DOI 10.1007/s00701-010-0874-4

LETTER TO THE EDITOR

Importance of distinction between paroxysmal and continuous patterns of pain during evaluation of pain after brachial plexus injury

Mohamed M. Aly · Youichi Saitoh · Haruhiko Kishima · Koichi Hosomi · Toshiki Yoshimine

Received: 11 October 2010 / Accepted: 4 November 2010 / Published online: 20 November 2010

We read with great interest the manuscript of Bonilla et al. entitled "Pain and brachial plexus lesions: evaluation of initial outcomes after reconstructive microsurgery and validation of a new pain severity scale" [3]. The authors described a new pain scoring scale to quantify pain after brachial plexus injuries and used it to assess patients' pain before and after reconstructive surgery. Within this scale, [3] the authors integrated pain intensity scale (measured on a scale ranging from 0 to 10), with other parameters like the disability in daily activities and sleep, pain frequency, use of pain medication, and the number of zones affected by pain.

We agree with the authors that the use of such a multi-dimensional pain scale would be useful as a standard outcome measure across studies for BPA pain that would greatly enhance the comparability, validity, and clinical applicability of these studies. Whereas most of the available reports used pain intensity scales, such as the visual analogue scale as the sole outcome measure, the new pain scale integrated factors beyond changes in pain intensity which may be more objective and of more relevance to the patient outcome.

One limitation of the above-mentioned pain scale is that it did not distinguish between the different patterns of BPA pain. It is well known that BPA pain has two patterns which are quite distinct from each other in terms of frequency and pain quality [5, 6]. Continuous background pain is usually described as burning, throbbing, and/or aching sensations and continues for a long duration, whereas paroxysmal pain is usually described as "electrical shock" or "shooting" paroxysms and usually lasts only for a few seconds [5, 6]. Although the authors included pain frequency [3], described as no pain to continuous pain, in their pain scale, this may not be sufficient to allow distinction between the two types of pain. Instead, we suggest that pain character (burning vs shooting) be also included during evaluation [1, 4]. Each type of pain should be quantified separately using visual analogue scale [1, 4]. Separate rating for the two patterns of pain will be particularly useful in evaluating the outcome of neurosurgical procedures for BPA pain [1, 6], thereby allowing clinicians to study the differential effects of the procedures on pain. Sindou et al. reported that DREZotomy was more effective for paroxysmal than continuous pain [6]. They explained the differential effects of DREZotomy based on the distinct pain origin for each type of pain [6]. Paroxysmal pain is said to originate from hyperactive neurons in the dorsal horn, whereas continuous pain extend beyond the dorsal horn up to the thalamus [6]. Also recently, our group reported that electrical motor cortex stimulation was more effective for continuous than paroxysmal pain [1]. Therefore, it can be said that pain classification is important to appropriately select patients

Electronic supplementary material The online version of this article (doi:10.1007/s00701-010-0874-4) contains supplementary material, which is available to authorized users.

M. M. Aly · Y. Saitoh (✉) · H. Kishima · K. Hosomi · T. Yoshimine
Department of Neurosurgery,
Osaka University Graduate School of Medicine,
2-2 Yamadaoka,
Suita 565-0871, Japan
e-mail: saitoh@nsurg.med.osaka-u.ac.jp

M. M. Aly · Y. Saitoh · H. Kishima · K. Hosomi · T. Yoshimine
Department of Neuromodulation and Neorosurgery,
Center of Advanced Science and Innovation, Osaka University,
Osaka University Graduate School of Medicine,
2-2 Yamadaoka,
Suita 565-0871, Japan

for treatment and to better understand the underlying mechanisms of pain as well [1, 4]. Finally, such distinction goes in line with several previous reports which have emphathized that classifying neuropathic pain, according to their different components, will help to develop a mechanism-based treatment [2].

Conflicts of interest None.

References

1. Aly MM, Saitoh Y, Oshino S, Hosomi K, Kishima H, Morris S, Shibata M, Yoshimine T. Differential efficacy of electrical motor cortex stimulation and lesioning of the dorsal root entry zone for continuous versus paroxysmal pain after brachial plexus avulsion. Neurosurgery (In Press)
2. Attal N, Fermanian C, Fermanian J, Lanteri-Minet M, Alchaar H, Bouhassira D (2008) Neuropathic pain: are there distinct subtypes depending on the aetiology or anatomical lesion? Pain 138(2):343–353
3. Bonilla G, Di Masi G, Battaglia D, Otero JM, Socolovsky M (2010) Pain and brachial plexus lesions: evaluation of initial outcomes after reconstructive microsurgery and validation of a new pain severity scale. Acta Neurochir (Wien) doi:10.1007/s00701-010-0709-3
4. Bouhassira D, Attal N, Fermanian J, Alchaar H, Gautron M, Masquelier E, Rostaing S, Lanteri-Minet M, Collin E, Grisart J, Boureau F (2004) Development and validation of the neuropathic pain symptom inventory. Pain 108:248–257
5. Parry CB (1984) Pain in avulsion of the brachial plexus. Neurosurgery 15:960–965
6. Sindou M, Blondet E, Emery E (2005) Microsurgical lesioning in the dorsal root entry zone for pain due to brachial plexus avulsion: a prospective series of 55 patients. J Neurosurg 102:1018–1028

NeuroImage 49 (2010) 2564–2569

Contents lists available at ScienceDirect

NeuroImage

journal homepage: www.elsevier.com/locate/ynimg

Modulation of neuronal activity after spinal cord stimulation for neuropathic pain; $H_2{}^{15}O$ PET study

Haruhiko Kishima [a], Youichi Saitoh [a,*], Satoru Oshino [a], Koichi Hosomi [a], Mohamed Ali [a], Tomoyuki Maruo [a], Masayuki Hirata [a], Tetsu Goto [a], Takufumi Yanagisawa [a], Masahiko Sumitani [d], Yasuhiro Osaki [b], Jun Hatazawa [c], Toshiki Yoshimine [a]

[a] Department of Neurosurgery, Osaka University, Graduated school of Medicine, Suita, Osaka, Japan
[b] Otorhinolaryngology, Osaka University, Graduated school of Medicine, Suita, Osaka, Japan
[c] Nuclear Medicine and Tracer Kinetics, Osaka University, Graduated school of Medicine, Suita, Osaka, Japan
[d] Department of Anesthesiology and Pain Relief Center, The University of Tokyo Hospital, Tokyo, Japan

ARTICLE INFO

Article history:
Received 8 July 2009
Revised 27 September 2009
Accepted 19 October 2009
Available online 27 October 2009

Keywords:
Neuropathic pain
Spinal cord stimulation
Regional cerebral blood flow

ABSTRACT

Spinal cord stimulation (SCS) is an effective therapy for chronic neuropathic pain. However, the detailed mechanisms underlying its effects are not well understood. Positron emission tomography (PET) with $H_2{}^{15}O$ was applied to clarify these mechanisms. Nine patients with intractable neuropathic pain in the lower limbs were included in the study. All patients underwent SCS therapy for intractable pain, which was due to failed back surgery syndrome in three patients, complex regional pain syndrome in two, cerebral hemorrhage in two, spinal infarction in one, and spinal cord injury in one. Regional cerebral blood flow (rCBF) was measured by $H_2{}^{15}O$ PET before and after SCS. The images were analyzed with statistical parametric mapping software (SPM2). SCS reduced pain; visual analog scale values for pain decreased from 76.1 ± 25.2 before SCS to 40.6 ± 4.5 after SCS (mean $\pm$ SE). Significant rCBF increases were identified after SCS in the thalamus contralateral to the painful limb and in the bilateral parietal association area. The anterior cingulate cortex (ACC) and prefrontal areas were also activated after SCS. These results suggest that SCS modulates supraspinal neuronal activities. The contralateral thalamus and parietal association area would regulate the pain threshold. The ACC and prefrontal areas would control the emotional aspects of intractable pain, resulting in the reduction of neuropathic pain after SCS.

Introduction

Neuropathic pain arises as a direct consequence of a lesion or disease affecting the somatosensory system (Loeser and Treede, 2008). It is generally more severe and more likely to be drug-resistant and persistent than nociceptive pain (Finnerup et al., 2005; Dworkin et al., 2003). Thus, chronic pain is often under-diagnosed and under-treated (Taylor, 2006), and it impairs quality of life. The causes of neuropathic pain vary and include such conditions as failed back surgery syndrome (FBSS), complex regional pain syndrome (CRPS), central post-stroke pain, phantom limb pain, peripheral and central nerve system injury, and post-spinal cord injury pain (Dworkin et al., 2003). Chronic neuropathic pain is most common in the back and legs.

Shealy et al. (1967) were the first to report that electrical stimulation of the dorsal spinal cord relieves cancer pain. Spinal cord stimulation (SCS) has since been applied not only to numerous cases of intractable pain but also to other conditions such as angina pectoris (AP), ischemic pain, and persistent vegetative state (Morita et al., 2007; Börjesson et al., 2008; Pedrini and Magnoni, 2007). Taylor (2006) reported that SCS not only reduces the pain but also improves quality of life in patients with FBSS or CRPS. He also reported that SCS is a cost-saving therapy. Kumar et al. (2007) reported that SCS provides better pain relief than conventional medical management alone in FBSS patients, and this was supported by a multicenter trial (Manca et al., 2008). Furthermore, the European Federation of Neurological Society guidelines support the effect of SCS in patients with FBSS or CRPS (Cruccu et al., 2007). For the central pain (spinal cord or brain lesions), SCS was reported to have some effect for pain relief. Katayama et al. (2001) reported that 7% of post-stroke pain patients revealed pain reduction with SCS and Kumar et al. (2006) also reported that SCS relieved 79% of the chronic pain due to multiple sclerosis. Thus, SCS is an essential treatment for relief of chronic neuropathic pain.

Oakley and Prager (2002) investigated some of the mechanisms underlying relief of pain by SCS. SCS was shown to stimulate the neurons of the dorsal horn of the spinal cord to release increased amount of acetylcholine and GABA and decreased amounts of aspartate and glutamate in rat models (Meyerson and Linderoth,

* Corresponding author. Department of Neurosurgery, Osaka University Faculty of Medicine, 2-2 Yamadaoka, Suita, 565-0871, Japan.
E-mail address: neurosaitoh@mbk.nifty.com (Y. Saitoh).

1053-8119/$ – see front matter © 2009 Elsevier Inc. All rights reserved.
doi:10.1016/j.neuroimage.2009.10.054

2000; Schechtmann et al., 2008). SCS was also shown to induce neurophysiological change, normalizing neuronal hyperexcitability in the dorsal horn (Yakhnitsa et al., 1999). In addition to these spinal mechanisms, functional alteration at the supraspinal level has been suggested to play an important role in pain reduction. Physiological study revealed cortical modulation during SCS (Polácek et al., 2007; Schlaier et al., 2007). However, the mechanism of pain relief by SCS is not fully understood. Brain activation during SCS has been analyzed by means of $H_2{}^{15}O$ positron emission tomography (PET) in patients with AP (Hautvast et al., 1997) and by means of functional magnetic resonance imaging (fMRI) in patients with FBSS (Kiriakopoulos et al., 1997; Stancák et al., 2008).

The investigators reported that SCS activates the primary and secondary sensorimotor cortex, cingulate cortex, insula, thalamus, and premotor cortex. Pain relief continues for several hours after SCS, so most patients with chronic pain use SCS intermittently, for example, several times per day. The modulation of brain activity after SCS has not been thoroughly examined.

In the present study, we used $H_2{}^{15}O$ PET to investigate the pattern of SCS-related neuronal activation and/or attenuation before and after SCS. $H_2{}^{15}O$ PET visualizes regional cerebral blood flow (rCBF), which reflects focal neuronal activation (Kapur et al., 1994). We also used statistical parametric mapping of normalized brain images to identify functionally specialized brain responses.

Materials and methods

Patients and surgical procedure

Nine patients (six men and three women) with intractable neuropathic pain in their lower extremities were included in this study (Table 1). Patients ranged in age from 28 to 65 years. The intractable neuropathic pain was due to FBSS in three patients, CRPS in two, cerebral hemorrhage in two, spinal cord infarction in one, and spinal cord injury in one. Pain was left-sided in five patients, right-sided in two patients, and bilateral in two patients. One of two patients with bilateral pain (patient 3) had more severe pain in right leg and the other (patient 8) had more severe pain in left leg. Their purposes of SCS were to reduce the pain in the more painful leg. Medical therapy had not been satisfactory, and the nine patients suffered from the intractable pain for 31 to 147 months before SCS was tried. Five of the nine patients showed slight to moderate motor weakness, and all had slight to severe sensory disturbance in the affected legs (Table 1). A visual analog scale (VAS), ranging from 0 to 100, and the short form of the McGill Pain Questionnaire (SF-MPQ) were used to evaluate the degree of pain.

The standard surgical procedure was used to place the SCS lead. In brief, under local anesthesia, a quadripolar electrode lead (Pisces Quad, 3487A; Medtronic, Inc., Minneapolis, MN, USA) was inserted percutaneously into the epidural space of the lumbar or thoracic spine by fluoroscopic guidance. The electrode was finally positioned after electrical sensation was detected in the region of pain upon stimulation. After confirmation of pain reduction in response to stimulation for 5–10 days, the electrode was connected to a subcutaneously implanted stimulator (Itrel III; Medtronic, Inc.).

Habitual bipolar stimulation was used for pain relief, and stimulation parameters varied between patients. General stimulation parameters were as follows: voltage, max 10 V; frequency, 10–85 Hz; pulse width, 210 to 450 μs; and duration of stimulation, 30 min. The patients controlled the stimulation at will and used SCS for at least 6 months before the PET study.

PET scanning procedure and activation task

The PET study was performed 6 to 12 months after implantation of the stimulation electrode. A Headtome-V PET scanner (Shimadzu, Kyoto, Japan) was used to scan in the three-dimensional acquisition mode with a shield to protect against scattered rays. Patients went without spinal cord stimulation for more than 12 h before the PET study. The patients lay with eyes closed in a silent and dim room. A 15-min transmission scan was acquired first with ^{68}Ge sources to correct for γ-ray attenuation. Relative CBF was measured based on the distribution of radioactivity after a slow bolus i.v. injection of $H_2{}^{15}O$ (7 mCi/scan, each lasting 90 s). Six PET scans corresponding to six $H_2{}^{15}O$ injections were obtained before SCS, SCS was performed for 30 min under the habitual condition, and six PET scans were obtained after pain reduction was confirmed. The PET protocol was the same as the motor cortex stimulation (MCS) protocol described previously (Kishima et al., 2007).

Data analysis

Attenuation-corrected data were reconstructed into an image (voxel sizes, $2 \times 2 \times 3.125$ mm; field of view, $256 \times 256 \times 196$ mm) with a resulting resolution of $4 \times 4 \times 5$ mm at FWHM (full width at half maximum). The images were analyzed with statistical parametric mapping (SPM) software (SPM2; Wellcome Department of Cognitive Neurology, London, UK) (Friston et al., 1991). PET images were anatomically normalized to fit with ICBM coordinates of the Montreal Neurological Institute. Images from each patient were realigned to the first volume of PET images and normalized to the template (Friston et al., 1995a) to account for variation in gyral anatomy and inter-individual variability in the structure–function relation and to improve the signal-to-noise ratio. This procedure was used for image realignment, anatomic normalization, smoothing (12 mm at FWHM), and statistical analysis (Kiebel et al., 1997). Data were normalized to global blood flow (average = 50). State-dependent differences in global blood flow were subjected to ANCOVA.

All nine patients were included in the same statistical analyses, with voxel-to-voxel comparison. Statistical parametric maps (SPM) were generated with an ANOVA model with the General Linear Model formulation of SPM2 (Friston et al., 1995b). We analyzed the main effect of SCS by comparing images obtained after SCS with those

Table 1
General characteristics of patients with deafferentation pain.

Patient	Age (years), sex	Etiology of pain	Pain laterality	Motor (0–5)	Sensory (0–10)	Duration of pain (months)	Pre-SCS VAS	Post-SCS VAS
1	44, M	Spinal infarction	Rt	4	4	36	80	40
2	60, F	Putaminal hemorrhage	Lt	4	10	99	100	55
3	65, F	FBSS	Bi (Rt > Lt)	5	10	147	90	30
4	45, M	CPRS	Lt	2	2	65	60	20
5	41, M	FBSS	Rt	3	5	54	85	25
6	28, F	CRPS	Lt	2	2	31	70	60
7	59, M	Putaminal hemorrhage	Lt	5	1	59	55	50
8	50, M	Spinal injury	Bi (Rt < Lt)	5	6	42	60	40
9	38, M	FBSS	Lt	5	10	57	85	45

FBSS, failed back surgery syndrome; CRPS, complex regional pain syndrome; Rt, right; Lt: left; Bi, bilateral; Motor, MMT score (0, complete paresis; 5, normal); Sensory, sensory scores (0, anesthesia; 10, normal); Pre-SCS VAS, VAS of pre-SCS; Post-SCS VAS, VAS of post-SCS.

Table 2
Increased rCBF after SCS.

Area	Cluster		Talairach coordinates (*x*, *y*, *z* mm)	Voxel equiv. *Z*
	p (corrected)	Size (voxels)		
(A) Rt thalamus	0.006	197	11.9, −15.6, 0.0	4.64
(B) Rt orbitofrontal (BA11)	0.040	161	43.6, 51.8, −12.7	4.70
(C) Lt Inf. parietal (BA7)	0.009	178	−33.7, −61.8, 45.5	4.39
(D) Rt Sup. parietal (BA7)	0.014	158	37.6, −45.9, 53.9	4.57
(E) Lt anterior cingulate (BA24)	0.001	301	−7.98, 38.1, 23.4	4.64
(F) Lt dorsolateral prefrontal (BA10)	0.050	100	−33.7, 36.0, 18.4	4.27

Rt, right; Lt, left; Inf, inferior; Sup, superior.

obtained before SCS, with the statistical threshold set at $p<0.02$ (corrected for multiple comparisons) in False Discovery Rate (FDW) for peak height, corrected for spatial extent (>8 voxels per cluster), and the cluster size was set at 100 contiguous voxels.

This method was used to generate SPM (*t*) of rCBF changes associated with each comparison. For between-group comparisons, the SPM (*t*) maps were transformed into SPM (*z*), and the levels of significance of areas of activation were assessed according to the peak height of foci estimation based on the theory of random Gaussian fields.

Three patients had been treated to reduce the right lower limb pain (patients 1, 3, and 5). MRIcro (http://www.sph.sc.edu/comd/rorden/mricro.html) was used to invert the images obtained from these patients from the right to the left so that statistical analysis would be consistent with that of other patients. The images were then realigned, normalized, and analyzed as previously described. Furthermore, to detect the correlation of the rCBF change and SCS efficacy, these images were performed covariance analysis with the VAS reduction rate after SCS ((pre-VAS − post-VAS) / pre-VAS).

Significance was accepted if a cluster showed a cluster corrected threshold of $p<0.05$. Anatomical locations were indicated according to the atlas of Talairach and Tournoux (1988).

This study adhered to the guidelines of the Declaration of Helsinki on the use of human subjects in research, and the patients provided written informed consent. This study was approved by the ethics committee of Osaka University Hospital.

Results

Pain reduction after SCS

After SCS, all nine patients showed various degrees of pain reduction according to VAS data (76.1 ± 25.2 to 40.6 ± 4.5) (Table 1). The pain reduction began during SCS and continued for at least 120 min after SCS. The degree of pain reduction remained stable for 60 min during the post-SCS PET scanning phase. In general, results of the SF-MPQ were for the most part compatible with VAS scores.

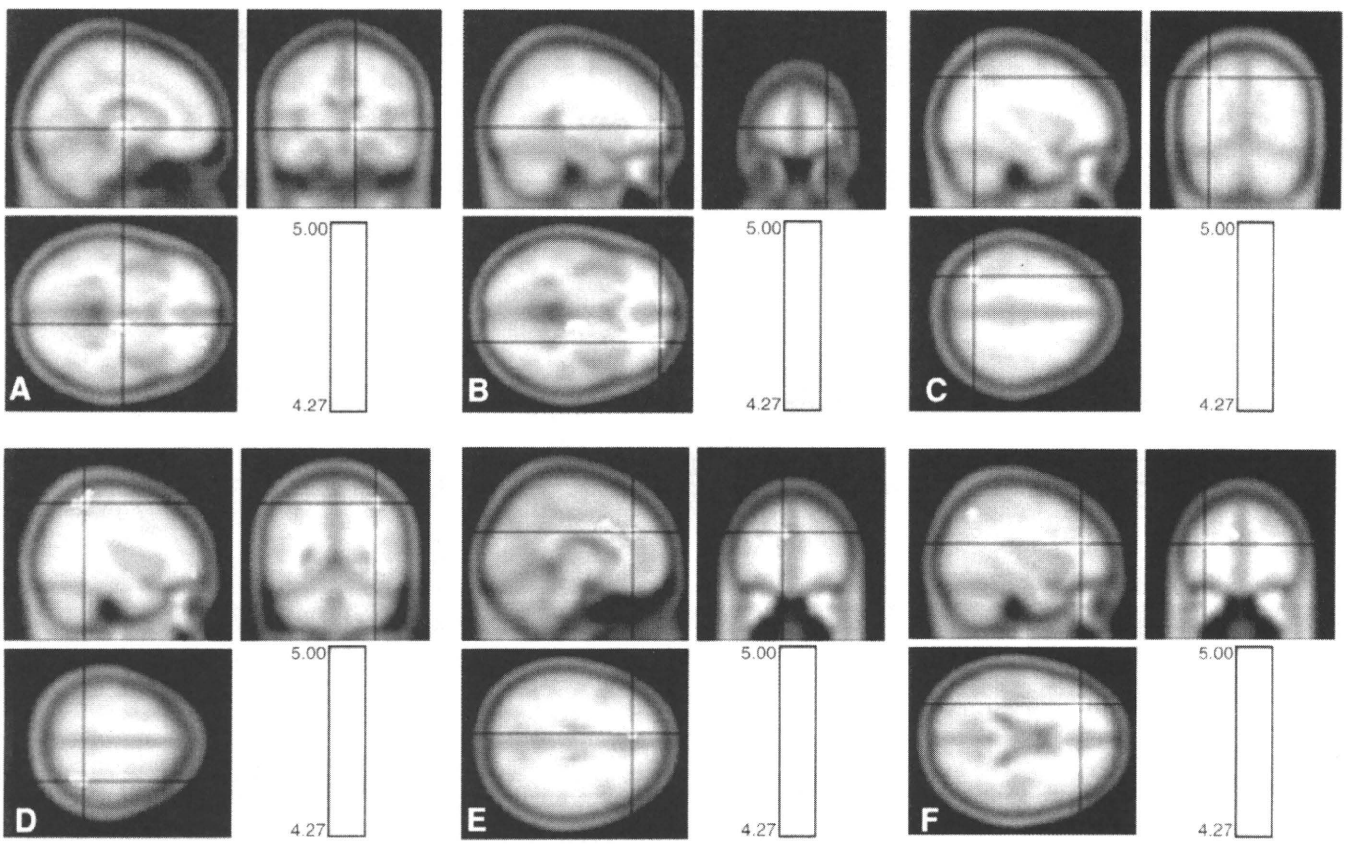

Fig. 1. Statistical parametric maps (*Z* maps) of intensity in normalized images. Comparison of rCBF before and after SCS shows that rCBF is increased after SCS in the right thalamus (A), right orbitofrontal cortex (BA11) (B), left inferior parietal lobule (C), right superior parietal lobule (D), left anterior cingulate cortex (E), and left dorsolateral prefrontal cortex (F). Colored bar indicates *Z* value (threshold, $p<0.05$). Panels A–F correspond to Table 2.

Table 3
Increased rCBF after SCS in reference to the affected side.

Area	Cluster		Talairach coordinates (*x*, *y*, *z* mm)	Voxel equiv. *Z*
	p (corrected)	Size (voxels)		
(A) C. Inf. parietal (BA40)	0.002	207	30.9, −47.9, 53.5	5.48
(B) C. Inf. parietal (BA40)	0.003	432	43.2, −46.0, 30.8	4.96
(C) C. dorsolateral prefrontal (BA10)	0.004	169	25.6, 56.8, 6.2	4.78
(D) C. anterior cingulate (BA24)	0.005	183	8.0, 18.0, 30.6	4.55
(E) I. lateral precentral (BA6)	0.01	109	−46.6, 0.6, 10.3	4.22
(F) C. thalamus	0.011	108	8.0, −16.9, −1.14	4.17
(G) I. dorsolateral prefrontal (BA9)	0.013	128	−27.2, 25.8, 25.7	4.06
(H) I. orbitofrontal (BA10)	0.014	143	−34.2, 43.2, −8.6	4.02
(I) I. Sup. parietal (BA7)	0.018	127	−27.2, −67.3, 35.0	3.85

I, ipsilateral to affected side; C, contralateral to affected side; Bi, bilateral; Inf, inferior; Sup, superior.

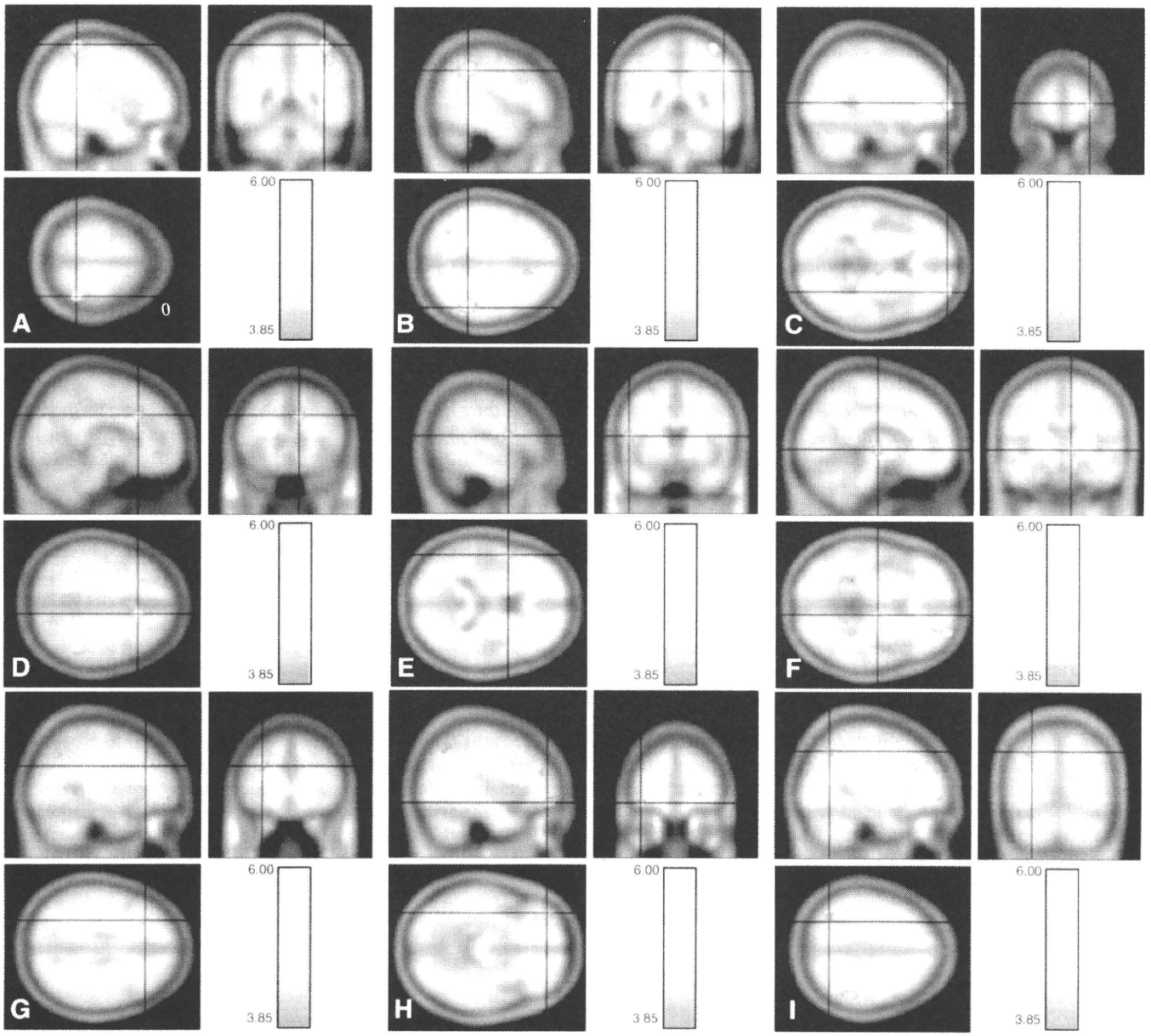

Fig. 2. Statistical parametric maps (*Z* maps) of intensity in normalized images. Comparison of rCBF before and after SCS by positioning the affected sides on the left shows that rCBF is increased after SCS in the contralateral inferior parietal lobules ($Z = 5.48$, 4.96) (A, B), contralateral dorsolateral prefrontal cortex (BA10) ($Z = 4.78$) (C), contralateral anterior cingulate cortex (BA24) ($Z = 4.55$) (D), contralateral orbitofrontal cortex (BA10) ($Z = 4.63$) and contralateral medial prefrontal cortex (BA10) ($Z = 4.56$), ipsilateral lateral precentral cortex (BA6) ($Z = 4.22$) (E), contralateral thalamus ($Z = 4.17$) (F), ipsilateral dorsolateral prefrontal (BA9) ($Z = 4.06$) (G), ipsilateral orbitofrontal cortex (BA10) ($Z = 4.02$) (H), and ipsilateral superior parietal lobule (BA7) ($Z = 3.85$) (I). Colored bar indicates *Z* value. Colored bar indicates *Z* value (threshold, $p < 0.05$). Panels A–I correspond to Table 3.

Brain activation profiles in response to SCS

Comparison of rCBF before and after SCS showed significant rCBF increases in the right thalamus ($Z=4.64$), right orbitofrontal cortex (BA11) ($Z=4.70$), left inferior parietal lobule (BA7) ($Z=4.39$), right superior parietal lobule (BA7) ($Z=4.57$), and left anterior cingulate cortex (ACC) (BA24) ($Z=4.64$), and left lateral prefrontal cortex (BA10) ($Z=4.27$) (Table 2, Fig. 1). There was no region where rCBS decreased after SCS.

The result analyzed after three images of patients 1, 3, and 5 were inverted so that the affected side appeared on the left, showed that rCBF was increased in the contralateral (right) inferior parietal lobules ($Z=5.48$, 4.96), contralateral dorsolateral prefrontal cortex (BA10) ($Z=4.78$), contralateral ACC (BA24) ($Z=4.55$), contralateral thalamus ($Z=4.17$), and ipsilateral lateral precentral cortex (BA6) ($Z=4.22$), dorsolateral prefrontal (BA9) ($Z=4.06$), ipsilateral orbitofrontal cortex (BA10) ($Z=4.02$), and ipsilateral superior parietal lobule (BA7) ($Z=3.85$) (Table 3, Fig. 2). There was no region where rCBF decreased after SCS. When these images were performed covariance analysis with VAS reduction rate after SCS, increased rCBF in ipsilateral dorsolateral prefrontal cortex (BA9) ($Z=5.59$), ipsilateral lateral precentral cortex (BA6) ($Z=5.18$), ipsilateral medial prefrontal cortex (BA8) ($Z=4.08$), and contralateral medial prefrontal cortex (BA8) ($Z=4.18$) were positively correlated with pain reduction rate (Table 4, Fig. 3).

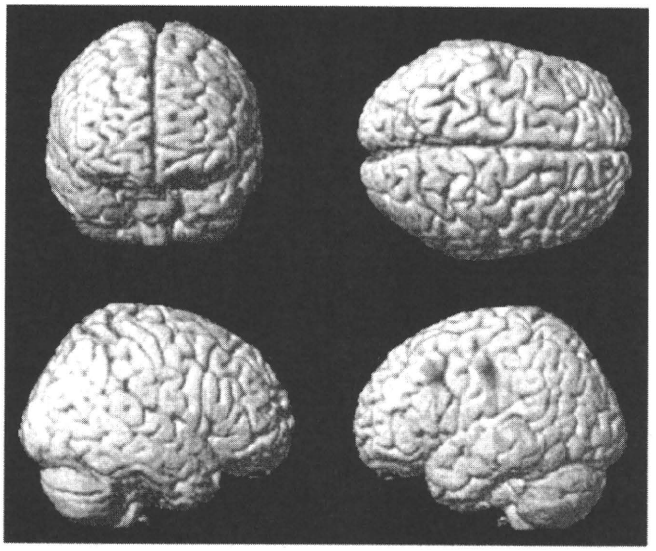

Fig. 3. Areas of significantly increased rCBF correlated to the VAS reduction rate after SCS, rendered in the normalized images, indicate ipsilateral to affected side of dorsolateral prefrontal cortex (BA9), ipsilateral lateral precentral cortex (BA6), and bilateral medial prefrontal (BA8) (threshold, $p<0.05$).

Discussion

This is the first report that rCBF is modified after SCS for chronic neuropathic pain as shown by $H_2{}^{15}O$ PET. rCBF is thought to reflect focal neuronal activation (Kapur et al., 1994). Thus, we concluded that there is a change in neuronal activation after SCS in patients with neuropathic pain. Our study included nine patients who underwent SCS to relieve their neuropathic pain. Although the etiology of chronic pain varied, all nine patients experienced some pain relief with SCS, and all used SCS everyday for more than several months. So we categorized them as SCS responders based on their pain reduction, and we report that the observed rCBF changes may be involved in the pain relieving mechanism of SCS.

We measured neuronal activity with $H_2{}^{15}O$ PET before and after SCS, and all PET images were normalized and then analyzed by SPM (Friston et al. 1991; 1995a,b; Kiebel et al., 1997). Therefore, the results of this study were based on anatomically well-standardized samples. Furthermore, images of three patients having only right-sided pain were reversed to move the affected side to the left and were analyzed with the others. This method statistically enhances the results, especially in pain cognition-related regions.

We found that rCBF increased in the right thalamus and superior parietal lobule (BA7) and left inferior parietal lobule (BA7) after SCS. rCBF was also shown to be increased in the contralateral thalamus and contralateral inferior parietal lobule (BA40), and ipsilateral superior parietal lobule (BA7) when we moved the affected side to the left. BA7 is the secondary somatosensory area (S2), and BA40 is the parietal association area. These areas play important roles for cognition of the somatosensory input.

One interesting finding of this study is that neither the contralateral primary motor cortex (M1) nor S1 corresponding to the affected leg showed rCBF change after SCS. This finding is contrary to previous reports that the contralateral S1 and the contralateral paracentral regions are activated during SCS as shown by electrophysiological methods (Polácek et al., 2007) and fMRI (Stancák et al., 2008). We attribute this difference to the fact that we performed PET scanning before and after SCS rather than during SCS as in the previous studies. During SCS, the patient often feels a stimulating sensation, and this might influence S1. After SCS, this sensation might diminish quickly; consequently, activation of S1 and paracentral regions would normalize. Moreover, the pain relief continues for several hours after SCS. Thus, S2 and the parietal association area are modulated by SCS and would control the threshold of the chronic pain for several hours after SCS.

An important finding is that the contralateral thalamus was shown to be activated in the post-SCS phase after the affected side was adjusted to the left. This finding is contrary to that of a previous report based on fMRI that did not describe thalamic activation during SCS (Stancák et al., 2008). It is also reported that the thalamus contralateral to the painful side shows hypometabolism in cases of central pain (De Salles and Bittar, 1994; Laterre et al., 1998). Hsieh et al. (1995) reported that rCBF in the contralateral thalamus was decreased by the peripheral nerve block with lidocaine in the mononeuropathy patients. We suppose this method might inhibit the sensory input of the peripheral to spinal cord and it might reduce the spino-thalamic information, resulting to the reduction of the contralateral thalamic activity. In our study, however, SCS never blocks the sensory input and it just controls the pain. So the result in this study is different from the previous report of Hsieh et al. Although the detailed role of the contralateral thalamus in the pathology of

Table 4
Increased rCBF after SCS covariate with pain reduction rate.

Area	Cluster		Talairach coordinates (x, y, z mm)	Voxel equiv. Z
	P (corrected)	Size (voxels)		
(A) I. dorsolateral prefrontal (BA9)	0.001	396	−44.8, 14.1, 32.1	5.59
(B) I. lateral precentral (BA6)	0.002	559	−44.8, −18.8, 34.0	5.18
(C) C. Sup. prefrontal (BA8)	0.008	168	13.3, 20.0, 53.6	4.18
(D) I. Sup. prefrontal (BA8)	0.01	112	−18.4, 14.1, 49.7	4.08

I, ipsilateral to affected side; C, contralateral to affected side; Bi, bilateral; Sup, superior.

neuropathic pain remains unclear, it is possible that SCS induces neuronal activity in contralateral thalamus, resulting in pain relief, and that the thalamus alters the pain threshold and sensory cognition after SCS, as previously reported (Garcia-Larrea et al., 1999).

It was shown that the ACC, dorsolateral prefrontal cortex, and orbitofrontal cortex were activated after SCS. The ACC and prefrontal cortex are reported to be involved in the modulation of pain and emotion. The activation of prefrontal cortex and ipsilatearl lateral precentral cortex was correlated with the degree of SCS efficacy (Table 4, Fig. 3). A previous report on MCS showed correlation between pain relief and ACC activation (Kishima et al., 2007; Peyron et al., 2007). Peyron et al. (2007) also reported that the prefrontal region, orbitofrontal region, and ACC act as descending (top–down) inhibitory controls for pain threshold in patients treated with MCS. Ochsner et al. (2004) reported that the prefrontal region and ACC recruit the up- and down-regulation of negative emotion. It has been reported that the activity of the right ventrolateral prefrontal region correlates with reduced negative emotional experience (Wager et al., 2008) and that fear of various types of physical pain predicts activation of the ventrolateral frontal region and anterior and posterior cingulate regions (Ochsner et al., 2006). Furthermore, because the ACC and prefrontal area are components of the brain reward system, it is possible that this system is also activated by SCS. In line with these findings, SCS itself and/or pain relief induced by SCS would control the emotional aspects of pain, resulting in a long lasting effect. The role of ipsilateral precentral area activated after SCS is not clear. The activation of dorsolateral prefrontal regions would reflect the most of the patients' satisfaction.

It was reported that rCBF increases to noxious stimuli are observed in S2, S1, thalamus, ACC, dorsal parietal, and prefrontal area (Peyron et al. 2000). SCS during heat stimuli increased rCBF in S2, S1, and posterior insula (Stancák et al. 2008). Thalamus, ACC, dorsal parietal, S2 and prefrontal regions were activated after SCS with neuropathic pain in this study. In line with those results, we could suppose that both acute pain stimuli and pain reduction by SCS would induce the neuronal activation in the similar regions. After SCS for patients with neuropathic pain, the change of sensory input, pain cognition, attention, and memory network would activate thalamus, parietal areas, ACC, and prefrontal areas.

Conclusions

For treatment of neuropathic pain, SCS controls pain cognition by modulating the thalamus and parietal association area. SCS also controls the emotional aspects of pain by modulating the prefrontal region and ACC. These findings support the use of SCS for treatment of neuropathic pain.

References

Börjesson, M., Andrell, P., Lundberg, D., Mannheimer, C., 2008. Spinal cord stimulation in severe angina pectoris–a systematic review based on the Swedish Council on Technology assessment in health care report on long-standing pain. Pain 140, 501–508.

Cruccu, G., Aziz, T.Z., Garcia-Larrea, L., Hansson, P., Jensen, T.S., Lefaucheur, J.P., Simpson, B.A., Taylor, R.S., 2007. EFNS guidelines on neurostimulation therapy for neuropathic pain. Eur. J. Neurol. 14, 952–970.

De Salles, A.A., Bittar Jr., G.T., 1994. Thalamic pain syndrome: anatomic and metabolic correlation. Surg. Neurol. 41, 147–151.

Dworkin, R.H., Backonja, M., Rowbotham, M.C., Allen, R.R., Argoff, C.R., Bennett, G.J., Bushnell, M.C., Farrar, J.T., Galer, B.S., Haythornthwaite, J.A., Hewitt, D.J., Loeser, J.D., Max, M.B., Saltarelli, M., Schmader, K.E., Stein, C., Thompson, D., Turk, D.C., Wallace, M.S., Watkins, L.R., Weinstein, S.M., 2003. Advances in neuropathic pain: diagnosis, mechanisms, and treatment recommendations. Arch. Neurol. 60, 1524–1534.

Finnerup, N.B., Otto, M., McQuay, H.J., Jensen, T.S., Sindrup, S.H., 2005. Algorithm for neuropathic pain treatment: an evidence based proposal. Pain 118, 289–305.

Friston, K.J., Frith, C.D., Liddle, P.F., Frackowiak, R.S., 1991. Comparing functional (PET) images: the assessment of significant change. J. Cereb. Blood Flow Metab. 11, 690–699.

Friston, K.J., Ashburner, J., Poline, J.B., Frith, C.D., Heather, J.D., Frackowiak, R.S.J., 1995a. Spatial registration and normalization of images. Hum. Brain Mapp. 2, 165–189.

Friston, K.J., Holmes, A.P., Worsley, K.J., Poline, J.P., Frith, C.D., Frackowiak, R.S.J., 1995b. Statistical parametric maps in functional imaging: a general linear approach. Hum. Brain Mapp. 2, 189–210.

Garcia-Larrea, L., Peyron, R., Mertens, P., Gregoire, M.C., Lavenne, F., Le Bars, D., Convers, P., Mauguière, F., Sindou, M., Laurent, B., 1999. Electrical stimulation of motor cortex for pain control: a combined PET-scan and electrophysiological study. Pain 83, 259–273.

Hautvast, R.W., Ter Horst, G.J., DeJong, B.M., DeJongste, M.J., Blanksma, P.K., Paans, A.M., Korf, J., 1997. Relative changes in regional cerebral blood flow during spinal cord stimulation in patients with refractory angina pectoris. Eur. J. Neurosci. 9, 1178–1183.

Hsieh, J.C., Belfrage, M., Stone-Elander, S., Hansson, P., Ingvar, M., 1995. Central representation of chronic ongoing neuropathic pain studied by positron emission tomography. Pain 63, 225–236.

Katayama, Y., Yamamoto, T., Kobayashi, K., Kasai, M., Oshima, H., Fukaya, C., 2001. Motor Cortex stimulation for post-stroke pain: comparison of spinal cord and thalamic stimulation. Stereotact. Funct. Neurosurg. 77, 183–186.

Kapur, S., Meyer, J., Wilson, A.A., Houle, S., Brown, G.M., 1994. Activation of specific cortical regions by apomorphine: an [15O]H2O PET study in humans. Neurosci. Lett. 176, 21–24.

Kiebel, S.J., Ashburner, J., Poline, J.B., Friston, K.J., 1997. MRI and PET coregistration—a cross validation of statistical parametric mapping and automated image registration. NeuroImage 5, 271–279.

Kiriakopoulos, E.T., Tasker, R.R., Nicosia, S., Wood, M.L., Mikulis, D.J., 1997. Functional magnetic resonance imaging: a potential tool for the evaluation of spinal cord stimulation: technical case report. Neurosurgery 41, 501–504.

Kishima, H., Saitoh, Y., Osaki, Y., Nishimura, H., Kato, A., Hatazawa, J., Yoshimine, T., 2007. Motor cortex stimulation in patients with deafferentation pain: activation of the posterior insula and thalamus. J. Neurosurg. 107, 43–48.

Kumar, K., Hunter, G., Demeria, D., 2006. Spinal cord stimulation in treatment of chronic benign pain: challenges in treatment planning and present status, a 22-year experience. Neurosurgery 58, 481–496.

Kumar, K., Taylor, R.S., Jacques, L., Eldabe, S., Meglio, M., Molet, J., Thomson, S., O'Callaghan, J., Eisenberg, E., Milbouw, G., Buchser, E., Fortini, G., Richardson, J., North, R.B., 2007. Spinal cord stimulation versus conventional medical management for neuropathic pain: a multicentre randomised controlled trial in patients with failed back surgery syndrome. Pain 132, 179–188.

Laterre, E.C., De Volder, A.G., Goffinet, A.M., 1998. Brain glucose metabolism in thalamic syndrome. J. Neurol. Neurosurg. Psychiatry 51, 427–428.

Loeser, J.D., Treede, R.D., 2008. The Kyoto protocol of IASP basic pain terminology. Pain 137, 473–477.

Manca, A., Kumar, K., Taylor, R.S., Jacques, L., Eldabe, S., Meglio, M., Molet, J., Thomson, S., O'Callaghan, J., Eisenberg, E., Milbouw, G., Buchser, E., Fortini, G., Richardson, J., Taylor, R.J., Goeree, R., Sculpher, M.J., 2008. Quality of life, resource consumption and costs of spinal cord stimulation versus conventional medical management in neuropathic pain patients with failed back surgery syndrome (PROCESS trial). Eur. J. Pain 12, 1047–1058.

Meyerson, B.A., Linderoth, B., 2000. Mechanisms of spinal cord stimulation in neuropathic pain. Neurol. Res. 22, 285–292.

Morita, I., Keith, M.W., Kanno, T., 2007. Dorsal column stimulation for persistent vegetative state. Acta Neurochir., Suppl. 97 (Pt.1), 455–459.

Oakley, J.C., Prager, J.P., 2002. Spinal cord stimulation: mechanisms of action. Spine 27, 2574–2583.

Ochsner, K.N., Ray, R.D., Cooper, J.C., Robertson, E.R., Chopra, S., Gabrieli, J.D., Gross, J.J., 2004. For better or for worse: neural systems supporting the cognitive down- and up-regulation of negative emotion. NeuroImage 23, 483–499.

Ochsner, K.N., Ludlow, D.H., Knierim, K., Hanelin, J., Ramachandran, T., Glover, G.C., Mackey, S.C., 2006. Neural correlates of individual differences in pain-related fear and anxiety. Pain 120, 69–77.

Pedrini, L., Magnoni, F., 2007. Spinal cord stimulation for lower limb ischemic pain treatment. Interact. Cardiovasc. Thorac. Surg. 6, 495–500.

Peyron, R., Laurent, B., García-Larrea, L., 2000. Functional imaging of brain responses to pain. A review and meta-analysis (2000). Neurophysiol. Clin. 30, 263–288.

Peyron, R., Faillenot, I., Mertens, P., Laurent, B., Garcia-Larrea, L., 2007. Motor cortex stimulation in neuropathic pain. Correlations between analgesic effect and hemodynamic changes in the brain. A PET study. NeuroImage 34, 10–21.

Polácek, H., Kozák, J., Vrba, I., Vrána, J., Stancák, A., 2007. Effects of spinal cord stimulation on the cortical somatosensory evoked potentials in failed back surgery syndrome patients. Clin. Neurophysiol. 118, 1291–1302.

Schechtmann, G., Song, Z., Ultenius, C., Meyerson, B.A., Linderoth, B., 2008. Cholinergic mechanisms involved in the pain relieving effect of spinal cord stimulation in a model of neuropathy. Pain 139, 136–145.

Schlaier, J.R., Eichhammer, P., Langguth, B., Doenitz, C., Binder, H., Hajak, G., Brawanski, A., 2007. Effects of spinal cord stimulation on cortical excitability in patients with chronic neuropathic pain: a pilot study. Eur. J. Pain 11, 863–868.

Shealy, C.N., Mortimer, J.T., Reswick, J.B., 1967. Electrical inhabitation of pain by stimulation of the dorsal columns. Anesth. Analg. 46, 489–491.

Stancák, A., Kozák, J., Vrba, I., Tintera, J., Vrána, J., Polácek, H., Stancák, M., 2008. Functional magnetic resonance imaging of cerebral activation during spinal cord stimulation in failed back surgery syndrome patients. Eur. J. Pain 12, 137–148.

Taylor, R.S., 2006. Epidemiology of refractory neuropathic pain. Pain Pract. 6, 22–26.

Talairach, J., Tournoux, P., 1988. Coplanar Stereotaxic Atlas of the Human Brain. Thieme, Stuttgart.

Wager, T.D., Davidson, M.L., Hughes, B.L., Lindquist, M.A., Ochsner, K.N., 2008. Prefrontal–Subcortical pathways mediating successful emotion regulation. Neuron 59, 1037–1050.

Yakhnitsa, V., Linderoth, B., Meyerson, B.A., 1999. Spinal cord stimulation attenuates dorsal horn neuronal hyperexcitability in a rat model of mononeuropathy. Pain 79, 223–233.

Withstand Pressure of a Simple Fibrin Glue Sealant: Experimental Study of Mimicked Sellar Reconstruction in Extended Transsphenoidal Surgery

Satoru Oshino, Youichi Saitoh, Toshiki Yoshimine

BACKGROUND: **To examine the strength and tolerance of the fibrin glue sealant in a situation of extended transsphenoidal surgery. The withstand pressure of fibrin glue sealant was measured using a simple sellar reconstruction model.**

METHODS: **A 15-mm diameter hole at the bottom of a 51-cm high cylinder was covered with a Gore-Tex (Gore-Tex, Tokyo, Japan) sheet. A small plate was placed on the center for a brief fixation, and 3 mL of fibrin glue was applied over the entire bottom. Then water was gradually filled in five cylinders, and the water level at leakage was measured as withstand pressures at 10 minutes and 24 hours after sealant application. The stability of the sealant under pressures of 20 and 30 cm H_2O for 12 hours was also examined.**

RESULTS: **The median initial withstand pressure at 10 minutes was 32 cm H_2O ($n = 5$), and was significantly increased to 47.5 cm H_2O after 24 hours ($n = 4$). In four of five cylinders, fibrin glue sealants were stable against a pressure of 20 cm H_2O for 12 hours and 30 cm H_2O for the next 12 hours.**

CONCLUSIONS: **The withstand pressure of simple fibrin glue sealant without other biological reactions could be estimated to be more than 20 cm H_2O after application, and increased to more than 40 cm H_2O after 24hours. These data are practical for neurosurgeons to comprehend the strength and limit of fibrin glue sealant and suggests the importance to control the intracranial pressure to less than 20 cm H_2O, especially for the first 12 to 24 hours.**

Key words
- Cerebrospinal fluid leakage
- Extended transsphenoidal surgery
- Fibrin glue
- Withstand pressure

Abbreviations and Acronyms
CSF: Cerebrospinal fluid
ICP: Intracranial pressure
TSS: Transsphenoidal surgery

From the Department of Neurosurgery, Osaka University Graduate School of Medicine, Suita, Japan

To whom correspondence should be addressed: Youichi Saitoh, M.D., Ph.D. [E-mail: saitoh@nsurg.med.osaka-u.ac.jp]

Citation: World Neurosurg. (2010) 73, 6:701-704.
DOI: 10.1016/j.wneu.2010.04.001
*Journal homepage: **www.WORLDNEUROSURGERY.org***
*Available online: **www.sciencedirect.com***

INTRODUCTION

Prevention of postoperative cerebrospinal fluid (CSF) leakage is one of the most important challenges in skull base surgery including extended transsphenoidal surgery (TSS). Diverse methods of sellar reconstruction combining autograft tissue and biological or artificial materials have been developed to prevent this critical complication (2, 3, 7, 12). Fibrin glue is commonly applied at the end of procedures as a sealant. The layer of fibrin covers the reconstructed site and adheres to the surrounding tissue, particularly to the bone surface of the sphenoid sinus. In patients with large CSF fistulas, lumbar CSF drainage is also placed during the postoperative period, although in such cases the overflow pressure and duration of drainage can be determined only on an empirical basis (3). The watertight dural closure, even if ideal (6), is not always possible in clinical situations. We have had experience with several patients during their postsurgery TSS in whom we placed fascia to cover dural and bone defects, hooked autograft bone or silicon plate to the epidural space as a buttress, and applied fibrin glue to cover all of these (**Figure 1**); the same method was previously reported as "Gasket-Seal" closure (8). The CSF lumbar drainage has been placed for 5 to 7 days with an overflow pressure of 5 to 15 cm H_2O, depending on clinical condition, and fortunately there has not been permanent CSF leakage among these patients. Adhesion of fibrin glue to the bone surface is a major barrier to CSF, driven by intracranial pressure (ICP).

The withstand pressure of fibrin glue has been measured in neurosurgical fields using animal skin or dura mater with combinations of various biological materials (4, 10, 13). However, the strength of the attachment of fibrin glue sealant to hard tissue such as bone, which might exhibit relatively little biological reaction in the acute phase, has not been examined. To answer this basic question we measured the withstand pressure of fibrin glue sealant using a simple model of mimicked sellar reconstruction in extended TSS.

MATERIALS AND METHODS

A specially made 51-cm high plastic cylinder, which had an inside diameter of 15 mm and outside diameter of 20 mm, was used in this experiment (**Figure 2**). A round plate 5 mm in thickness and 40 mm in diameter consisting of epoxy-glass laminate was attached at the bottom of the cylinder, which had a hole 15 mm in diameter in the center continuing to the inner space of the cylinder. The hole at the bottom was closed using Gore-Tex sheets (JAPAN GORE-TEX Inc.; Tokyo, Japan), the plate (LactoSorb System, Walter Lorenz Surgical, Jacksonville, FL, USA), and fibrin glue (Beriplast P, CSL-Behring; Tokyo, Japan). The fibrin glue consisted of two components: solution A contained fibrinogen, factor XIII, and

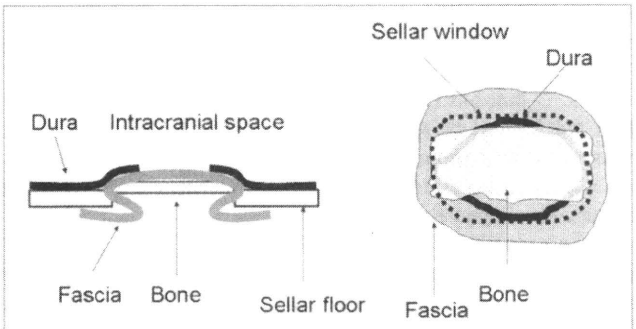

Figure 1. The method of our sellar reconstruction in extended-transsphenoidal surgery is shown. The fascia (thick gray line) is placed to cover the dural (thick black line) and bone defect (dotted column), and an autograft bone (square dotted line) is hooked to the epidural space as a buttress. Then fibrin glue is applied to cover all layers.

aprotinin, and solution B contained thrombin and calcium chloride.

Before the procedures, the surface of the epoxy-glass laminate was moistened with water as a substitute for CSF. Next, a round Gore-Tex sheet, 20 mm in diameter, was placed to cover the hole, and the plate (7 × 20 mm) was placed across the centre of the sheet as a buttress (**Figure 2**). The plate was then fixed using 5-mm wide gum tape to the side of the cylinder. Constructed in this fashion, both sleeves of the Gore-Tex sheet were free and not fixed. Then 3 mL of fibrin glue was applied over the entire surface of the bottom of the cylinder. To prevent overspilling of the fibrin glue, the outline of the bottom was yarded with 1-cm wide plastic tape, which was folded so that it did not emerge from the adhesion face inside. Solutions A and B were simultaneously applied manually using a Y-shaped attachment (Beriplast P Combi-Set, CSL-Behring; Tokyo, Japan). Care was taken to apply all 3 mL of the fibrin glue continuously and not to form multiple layers with it. This amount of glue was chosen to reduce variance in application compared with the preliminary examinations using 1 ml, in which conditions of fibrin glue coverage were not stable. A 10-minute interval was allowed for stabilization of the fibrin glue sealant. Then the cylinder was turned over and held in the air (**Figure 2**), and water carefully filled the cylinder along the inner wall at a slow rate of 1 cm per 5 seconds.

In experiment 1 (n = 5), the cylinder was filled with water until it leaked through the bottom. The water level at leakage was measured as the initial withstand pressure.

In experiment 2 (n = 5), the cylinder was initially filled with water to the 20-cm level, and water leakage was observed during the next 12 hours. After 12 hours, the water level was increased to the 30-cm level and observed for another 24 hours. At 24 hours, water was filled until it leaked, and the water level at leakage was considered the delayed withstand pressure.

RESULTS

Experiment 1

The initial withstand pressures at 10 minutes after sealant application were 35, 40, 32, 16, and 28 cm H_2O for each of the samples (**Figure 3A**). At leakage, the fibrin layer itself was not disrupted, but a part of it had been stripped from the bottom. Once the water began to leak, the fibrin layer surrounding the tract was immediately stripped from the bottom, forming a large tract for leakage.

Experiment 2

There was no leakage at the initial water level of 20 cm in any of the five cylinders. After 12 hours, the water level was the same, at 20 cm, in four cylinders, but had decreased to 7 cm in one cylinder. In that cylinder, although the sealant was not disrupted, small drops of water were detected around the sealant. The water level remained stable in the other four cylinders until 24 hours, even after filling to the 30-cm level. The delayed withstand pressures at 24 hours were 40, 47, 48, and 50 cm H_2O, which were significantly higher than the initial ones (n = 5) (**Figure 3**; $P < 0.05$, Mann Whitney U test).

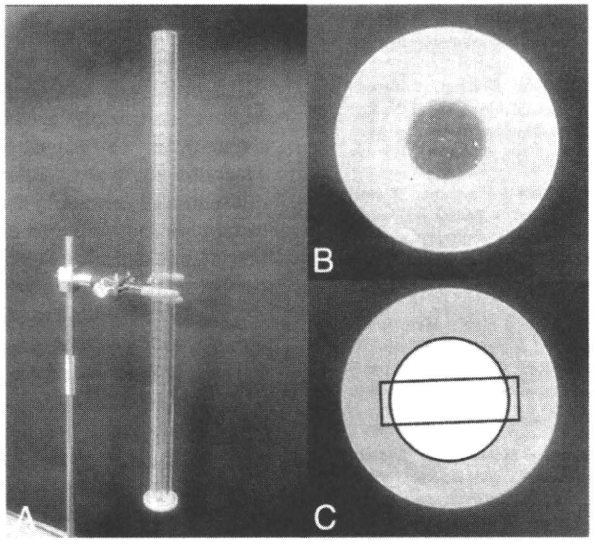

Figure 2. (**A**) A specially made 51-cm high plastic cylinder, which had an inside diameter of 15 mm and outside diameter of 20 mm, was used for the experiments. (**B**) A round plate 40 mm in diameter consisting of epoxy-glass laminate was attached to the bottom, which had a hole 15 mm in diameter. After the hole was covered with a round Gore-Tex sheet 20 mm in diameter and the 7 × 20 mm plate (**C**), the fibrin glue was applied over the entire bottom. The sheet and plate are outlined in black.

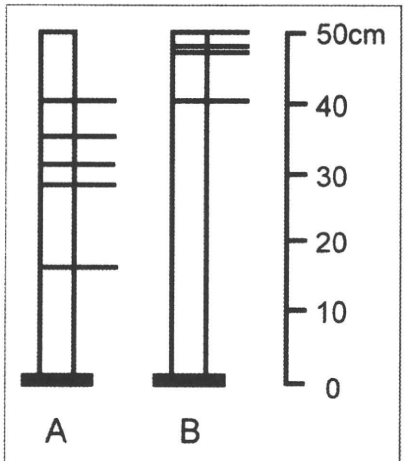

Figure 3. Withstand pressures of fibrin glue sealant at 10 minutes (**A**) and at 24 hours (**B**) after the application are shown. Because of water leakage in one cylinder at 12 hours, withstand pressures were measured in the remaining four cylinders at 24 hours. Withstand pressures at 24 hours were significantly higher than those at 10 minutes after the application ($P < 0.05$, Mann-Whitney U test).

DISCUSSION

Among the diverse methods of sellar reconstruction in endoscopic or extended TSS, fibrin glue has commonly been used as a sealant at the end of procedures (2, 3, 7, 8, 12). Fibrin glue has been used successfully in the management of wound healing or homeostasis in a wide range of surgeries (1). In the neurosurgical field, the withstand pressure of fibrin glue sealant has been studied in vitro for dural closure in craniotomy (10) or spinal surgery (4) and sellar closure in endoscopic TSS (13). In these studies, the burst pressures of fibrin sealant, which adhered to bovine dura mater or rabbit skin with a combination of suture (10) or biological materials such as polyglatine acid sheet (4, 13), were measured. In the present study, we mimicked the sellar reconstruction in extended TSS, in which the dural defect is only partially covered by materials, fixed by buttressing, and sealed with fibrin glue (8). We focused on the fact that fibrin glue adheres to the surrounding bone in TSS, which should exhibit relatively little biological reaction in the early postoperative period. In substitution for bone surface, we applied the epoxy-glass laminate, which has been widely used in nonanimal experiments as the imitation of bone (9, 11). Using other materials, such as hyroxyapatite, would have provided a more realistic model of the fibrin–bone interface, however, that was difficult for us because of technology and cost.

The results showed that, if fibrin glue is applied properly, a withstand pressure of more than 20 cm H_2O can be obtained at 10 minutes after application, and significantly increases with time to more than 40 cm H_2O after 24 hours. Similar findings have been reported in which the sealing effect of fibrin glue against alveolar air leakage in dogs was significantly increased to 70 cm H_2O after 24 hours from lower levels at 12 hours (5). We also found that the sealants were stable against a continuous pressure of 20 cm H_2O for the initial 12 hours and that of 30 cm H_2O for the following 12 hours. These data indicate that the control of ICP at less than 20 cm H_2O is especially important for the first 12 to 24 hours. The withstand pressure of 20 to 50 cm H_2O reflects the successful sellar reconstruction using fibrin glue without any special maneuver, even in case of incomplete dural closure, and is also reasonable as shown by CSF leakage after sudden elevation of ICP such as in severe sneezing or coughing.

As in extended TSS, we applied fibrin glue manually and did not use a spray kit in the present study. Although 3 mL was applied to each cylinder to reduce variance in coverage, one of five procedures (20%) in each experiment yielded exceptionally decreased withstand pressures. Technical errors during manual application may have resulted in contamination by air bubbles or formation of gaps between the fibrin layer and the surface of the laminate or within multiple fibrin layers. Technical improvement in application of fibrin glue to surgical gaps or defects will be important in increasing the strength of fibrin glue.

In clinical situations, additional factors such as oblique bone surface, impact of CSF pulse, continuous CSF flow during fibrin glue application and sudden variation in ICP must also be taken into account. However, we aimed to obtain the basic data about the strength of fibrin glue sealant before considering those variations. Our results provide unique information for neurosurgeons to comprehend the strength and also the limit of fibrin glue sealant and will be aid to develop the surgical method to prevent CSF leakage. It will be clinically interesting to perform the same experiments with other fibrin glue agents such as Tisseel (Baxter Corporation, Mississauga, Canada) or a recently developed sealant DURASEAL (Confluent Surgical Inc., Waltham, MA, USA) and compare those results, although both agents are not commercially available in Japan at present.

CONCLUSION

The withstand pressure of simple fibrin glue sealant was measured in a model of extended TSS. The initial withstand pressure was 32 cm H_2O at 10 minutes after application, and increased to more than 40 cm H_2O at 24 hours. Fibrin glue sealants were stable against a pressure of 20 cm H_2O for the initial 12 hours and 30 cm H_2O for the next 12 hours in 80% of cases. These practical data are important for neurosurgeons to comprehend the strength and also the limit of fibrin glue sealant. Technical improvement of fibrin glue application will be needed to make its effects more stable.

REFERENCES

1. Albala DM: Fibrin sealants in clinical practice. Cardiovasc Surg 11 Suppl 1:5-11, 2003.
2. Citardi MJ, Cox AJ, 3rd, Bucholz RD: Acellular dermal allograft for sellar reconstruction after transsphenoidal hypophysectomy. Am J Rhinol 14:69-73, 2000.
3. Esposito F, Dusick JR, Fatemi N, Kelly DF: Graded repair of cranial base defects and cerebrospinal fluid leaks in transsphenoidal surgery. Neurosurgery 60: 295-303 [discussion: 303-294], 2007.
4. Hida K, Yamaguchi S, Seki T, Yano S, Akino M, Terasaka S, Uchida T, Iwasaki Y: Nonsuture dural repair using polyglycolic acid mesh and fibrin glue: clinical application to spinal surgery. Surg Neurol 65:136-142 [discussion: 142-133], 2006.
5. Kawamura M, Gika M, Izumi Y, Horinouchi H, Shinya N, Mukai M, Kobayashi K: The sealing effect of fibrin glue against alveolar air leakage evaluated up to 48 h; comparison between different methods of application. Eur J Cardiothorac Surg 28:39-42, 2005.
6. Kitano M, Taneda M: Icing and multilayering technique of injectable hydroxyapatite cement paste for cranial base reconstruction after transsphenoidal surgery: technical note. Neurosurgery 61:E53-54 [discussion E54], 2007.
7. Laufer I, Anand VK, Schwartz TH: Endoscopic, endonasal extended transsphenoidal, transplanum transtuberculum approach for resection of suprasellar lesions. J Neurosurg 106:400-406, 2007.
8. Leng LZ, Brown S, Anand VK, Schwartz TH: "Gasket-seal" watertight closure in minimal-access en-

doscopic cranial base surgery. Neurosurgery 62 Suppl. 2:342-343, 2008.

9. Macdonald W, Carlsson LV, Gathercole N, Jacobsson CM: Fatigue testing of a proximal femoral hip component. Proc Inst Mech Eng H 217:137-145, 2003.

10. Nakajima S, Fukuda T, Hasue M, Sengoku Y, Haraoka J, Uchida T: New technique for application of fibrin sealant: rubbing method devised to prevent cerebrospinal fluid leakage from dura mater sites repaired with expanded polytetrafluoroethylene surgical membranes. Neurosurgery 49:117-123, 2001.

11. Pietrzak WS, Eppley BL: An experimental study of heat adaptation of bioabsorbable craniofacial meshes and plates. J Craniofac Surg 18:540-545, 2007.

12. Tamasauskas A, Sinkunas K, Draf W, Deltuva V, Matukevicius A, Rastenyte D, Vaitkus S: Management of cerebrospinal fluid leak after surgical removal of pituitary adenomas. Medicina (Kaunas) 44: 302-307, 2008.

13. Yano S, Tsuiki H, Kudo M, Kai Y, Morioka M, Takeshima H, Yumoto E, Kuratsu J: Sellar repair with resorbable polyglactin acid sheet and fibrin glue in endoscopic endonasal transsphenoidal surgery. Surg Neurol 67:59-64 [discussion 64], 2007.

Conflict of interest statement: The authors declare that the research was conducted in the absence of any commercial or financial relationships that could be construed as a potential conflict of interest.

received 19 November 2009; accepted 05 April 2010

Citation: World Neurosurg. (2010) 73, 6:701-704.
DOI: 10.1016/j.wneu.2010.04.001

Journal homepage: www.WORLDNEUROSURGERY.org

*Available online: **www.sciencedirect.com***

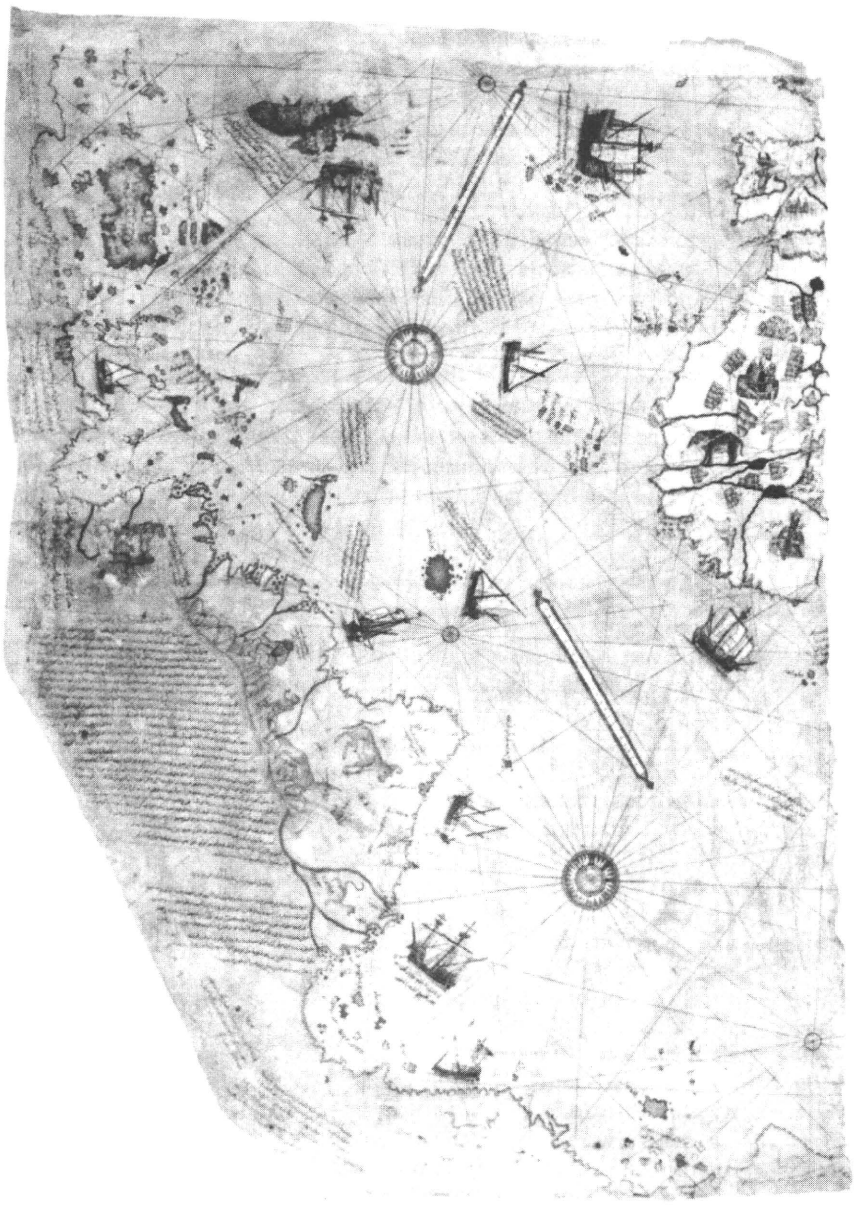

1513 map of the world by Hadji Muhiddin Piri Ibn Hadji Mehmed (ca. 1465 – ca. 1554), an Ottoman-Turkish Kaptan-ı Derya (Captain of the Sea, the equivalent of the modern Admiral of the Fleet), geographer, and cartographer.

Only a portion of the original map survives. The map synthesizes information from twenty maps, including one drawn by Christopher Columbus of the New World.

Courtesy of the Topkapi Museum, Istanbul, Turkey.

JOURNAL OF NEUROTRAUMA 27:403–410 (February 2010)

DOI: 10.1089/neu.2009.1044

Taurine Reduces Inflammatory Responses after Spinal Cord Injury

Yasuhiro Nakajima,[1] Koji Osuka,[2] Yukio Seki,[3] Ramesh C. Gupta,[4] Masahito Hara,[1] Masakazu Takayasu,[2] and Toshihiko Wakabayashi[1]

Abstract

Taurine has multiple functions in the central nervous system (CNS), serving as an osmoregulator, antioxidant, inhibitory neuromodulator, and regulator of intracellular Ca^{2+} flux. Since the role of taurine in traumatic spinal cord injury (SCI) is not fully understood, the present study was conducted with C57 black/6 mice (18–20 g) who underwent severe SCI at the Th-8 level using a weight compression device. Taurine was injected intraperitoneally at doses of 25, 80, 250, and 800 mg/kg within 30 min after SCI. Controls were injected with saline. The contusional cord segments were removed 6 h after SCI, and concentrations of interleukin-6 (IL-6) and myeloperoxidase (MPO) were measured using ELISA kits. Phosphorylation of STAT3, which is activated by IL-6, and expression of inducible cyclooxygenase-2 (COX-2) were also compared between the taurine treatment group (250 mg/kg) and the control group by Western blot analysis. Morphological changes were evaluated with H&E-stained sections. Taurine significantly decreased IL-6 and MPO levels in a dose-dependent manner, significantly reducing the phosphorylation of STAT3 and expression of COX-2 after SCI compared to controls. A reduced accumulation of neutrophils, especially in the subarachnoid spaces, and secondary degenerative changes in gray matter were also noted, and motor disturbances were significantly attenuated with taurine treatment (250 mg/kg). These findings indicate that taurine has anti-inflammatory effects against SCI, and may play a neuroprotective role against secondary damage, and thus it may have therapeutic potential.

Key words: interleukin-6; myeloperoxidase; spinal cord injury; taurine

Introduction

SPINAL CORD INJURY (SCI) often results in devastating permanent neurological deficits. Acute SCI not only causes early hemorrhagic necrosis, but also endothelial damage and marked reductions in microcirculation, leading to major infarctions at injury sites (Tator and Fehlings, 1991). Activated neutrophils migrate into necrotic regions after SCI (Carlson et al., 1998; Xu et al., 1990), and release a number of inflammatory cytokines such as interleukin-1 (IL-1), IL-6, and tumor necrosis factor-α (Hayashi et al., 2000; Pan et al., 2002; Streit et al., 1998; Wang et al., 1996a). SCI also increases levels of excitatory amino acids and causes oxidative stress, and all of these factors can contribute to progressive secondary injury. Currently, only high-dose methylprednisolone is advocated for the treatment of patients suffering from SCI (Bracken et al., 1990, 1997).

Taurine, 2-aminoethane sulfonic acid, is conditionally essential in humans and is ubiquitously expressed in many tissues. It acts as an antioxidant, osmoregulator, calcium regulator, and membrane stabilizer (Huxtable, 1992), and has been shown to be beneficial in the treatment of congestive heart failure (Azuma, 1994), ischemia-reperfusion injury (Milei et al., 1992), pulmonary fibrosis (Giri and Wang, 1992), and endothelial cell cytotoxicity (Wang et al., 1996b). Neutrophils contain high concentrations of taurine in their cytosol (Fukuda et al., 1982), and they play important roles in phagocytosis after SCI as a host defense mechanism against infection. However, the effects of taurine under pathophysiological circumstances, for example after SCI, have hitherto remained unclear (Gupta et al., 2006).

The purpose of the present study was thus to investigate any protective effects of exogenous taurine in a mouse spinal cord compression model. To elucidate its influence on

[1]Department of Neurosurgery, Nagoya University Graduate School of Medicine, Aichi, Japan.
[2]Department of Neurological Surgery, Aichi Medical University, Aichi, Japan.
[3]Department of Neurosurgery, Nagoya Daini Red Cross Hospital, Nagoya, Japan.
[4]School of Agricultural Sciences and Rural Development (SASRD), Nagaland University, Nagaland, India.

inflammatory responses, the IL-6 concentration, the degree of phosphorylation in an IL-6 signal transduction pathway, expression of inducible cyclooxygenase-2 (COX-2), and myeloperoxidase (MPO) level were all measured in injured spinal cords. We also examined the impact of taurine on hindlimb motor function after SCI.

Methods

Materials

Unless otherwise specified all chemicals were from Sigma Chemicals Co. Ltd. (St. Louis, MO).

Animals

Female mice (C57BL/6NCrj; Charles River Japan, Inc., Yokohama, Japan) 8–10 weeks of age (weight 18–20 g) were housed two or three per cage and kept at a temperature of 24°C with free access to water and food before and after surgery. The experiments were carried out in accordance with the National Institutes of Health guidelines for the care and use of laboratory animals, with approval of the appropriate committee of Nagoya University Graduate School of Medicine. All efforts were made to minimize the number of animals used and their suffering.

Spinal cord injury model and drug treatment

The mice were anesthetized with 1.5% halothane and maintained on 1.25% halothane in an oxygen/nitrous oxide (30%/70%) gas mixture. Temperature was monitored with rectal probes and maintained between 36.5° and 37.5°C with heating pads and lamps. The mice were fixed with a stereotaxic apparatus and subjected to severe spinal cord compression as previously described by Farooque (2000; Supplementary Fig. 1s) (see online supplementary material at http://www.liebertonline.com). In brief, laminectomy at the Th-8 vertebra was performed with the dura intact. Then 10 g/mm^2 of compression was applied to the exposed spinal cord for 5 min. After compression the skin incision was closed. Mice receiving laminectomy without compression were used as a sham-injury group. Taurine was administered as a single dose of 25, 80, 250, or 800 mg/kg by intraperitoneal injection within 30 min after SCI or sham surgery. Control mice received intraperitoneal injection of saline instead of taurine. The epicenters (2 mm in length) of SCI mice, and spinal cord (2 mm in length) of sham-injured mice were used as samples for analysis, and were collected after 6 h from mice under deep anesthesia killed by decapitation. The spinal cord tissues were frozen in liquid nitrogen and stored at −80°C until use.

Analysis of the IL-6 concentration and myeloperoxidase level

Spinal cord tissue samples for enzyme-linked immunosorbent assay (ELISA) were prepared using the following buffer: 10 mmol/L Tris-HCl (pH 8.0), 150 mmol/L sodium chloride, 1 mmol/L EDTA, 1 mmol/L PMSF, 1% Triton X-100, 10 μg/mL aprotinine, and 1 μg/mL pepstatin. Homogenates were centrifuged at 18,000*g* at 4°C for 15 min, and protein concentrations of the supernatants were determined by the method of Bradford using bovine serum as the standard. The concentration of IL-6 and MPO level were measured using sandwich ELISA kits (R&D Systems, Inc., Minneapolis, MN, and HyCult Biotechnology, Uden, The Netherlands, respectively), according to the manufacturer's instructions.

Analysis of phosphorylation of signal transducers and activators of transcription 3 (STAT3) and expression of COX-2 by Western blot analysis

Spinal cord tissue samples of each group were collected at 6 h after SCI and homogenized on ice in 300 μL of buffer and phosphatase inhibitor solution: 50 mmol/L Tris base/HCl (pH 7.5), 0.2 mmol/L EGTA (pH 7.5), 0.2 mmol/L EDTA (pH 8.0), 0.2 mmol/mL phenylmethylsulfonyl fluoride (PMSF), 1 μg/mL pepstatine, 0.2 μg/mL aprotinine, 2 μg/mL leupeptine, 0.1 mmol/L dithiothreitol, 1 mmol/L sodium orthovanadate (Na_3VO_4), 50 mmol/L sodium fluoride (NaF), 2 mmol/L sodium pyrophosphate ($Na_4P_2O_7 \cdot 10H_2O$), and 1% Nonidet P-40, for Western blot analysis. The homogenates were then centrifuged at 18,000*g* at 4°C for 15 min, and protein concentrations of the supernatants were determined by the method of Bradford using bovine serum as the standard. Crude supernatant samples containing 25 μg of protein were subjected to 7.5% SDS-PAGE, and the proteins were transferred to polyvinylidene difluoride (PVDF) membranes and incubated with primary antibodies against phosphorylated (*p*)- Tyr^{705}-STAT3 (Cell Signaling Technology, Inc., Beverly, MA) at a dilution of 1:500, actin at a dilution of 1:3000, and COX-2 (BD Biosciences Pharmingen, Franklin Lakes, NJ) at a dilution of 1:500, for 1 h at room temperature. After washing, the membranes were incubated with goat anti-rabbit polyclonal or anti-mouse monoclonal IgG conjugated to horseradish peroxidase at a dilution of 1:3000 for 30 min at room temperature. Reactions were developed with ECL (GE Healthcare, Buckinghamshire, U.K.). Phosphorylated-Tyr^{705}-STAT3 immunoblots were stripped from PVDF membranes and reblotted with primary antibodies against STAT3 (BD Biosciences Pharmingen) at a dilution of 1:500 for 1 h at room temperature. Exposure to the secondary antibody, goat anti-mouse monoclonal IgG, was at a dilution of 1:3000 for 30 min, followed by color development. Band intensities were quantitated by densitometric scanning using the NIH IMAGE program.

Histological examination of the spinal cord

Mice killed 6 h or 4 weeks after SCI were transcardially perfused with a phosphate-buffered solution of 10% formaldehyde. The spinal cord at Th-8 was then immediately removed and immersed overnight in the same solution. Transverse semi-serial paraffin-embedded sections 10 μm thick were prepared and stained with hematoxylin and eosin (H&E). An experienced pathologist blinded to study group assessed the sections.

Behavioral analysis

To investigate the effects of taurine on SCI, we measured recovery of hindlimb motor function using the Basso mouse scale (BMS) motor rating scale. Severe SCI mice were treated with taurine ($n = 6$; 250 mg/kg IP within 30 min after induction of SCI, and then once a day from day 1 until day 7), or saline ($n = 7$; IP on the same schedule). Two investigators observed each animal for 5 min and scored (0–9 scale) each